§21. Numerical Calculation of Emission Spectrum for Fast-ion Charge Exchange Spectroscopy

Kobayashi, S., Yamamoto, S., Mizuuchi, T. (IAE, Kyoto Univ.), Lee, H.Y. (KAIST), Nakamura, Y., Kirimoto, M., Harada, T., Yasueda, M., Lu, X. (GSES, Kyoto Univ.), Murakami, S. (Dep. Nucl. Eng., Kyoto Univ.), Nakashima, Y. (Univ. Tsukuba), Osakabe, M., Yokoyama, M., Sato, M., Kobayashi, M., Shoji, M., Ida, K., Yoshinuma, M.

In magnetically confined plasmas, it is important subject to estimate the velocity distribution of fast ions because it is strongly linked to the fast-ion-induced MHD instability and it provides the confinement characteristics of fast ions. Fast-ion charge exchange spectroscopy (FICXS) has been demonstrated in LHD to investigate the confinement property of the fast ions [1]. However, since the observed spectrum is summation of the cold component of H_α-line, halo and FICX components, simulation calculations and comparison with the experimental results are required to forecast the spatial and velocity distibution of fast-ion in the hot plasmas. In this study, we calculated the FICXS spectrum using a set of numerical calculation codes.

As shown in Fig. 1, a set of numerical calculations for FICXS spectrum consists of beam birthpoint analysis (HFREYA), estimation of the prompt loss and the re-distribution of beam ions using a drift orbit calculation (mcnbi), Fokker–Planck analysis (FIT, 0-dimensional (0D) in real spatial and 1D in velocity space), estimation of halo-neutral distribution using Monte-Carlo method and finally, spectrum calculation for FICXS. In this study, the spectrum calculation of FICXS was carried out in the case of the test geometry using the Heliotron J configuration. The left figure in Fig. 2 shows the 2D beam density profile for BL2 (co) and vacuum vessel of Heliotron J. Three candidates for the FICXS sightlines are denoted as A, B and C [2]. In this calculation, we assumed that the fast ions have a monotonic pitch angle of 155 degree. The 1D velocity distribution of fast ions calculated by the Fokker–Planck analysis is shown in the right figure of Fig. 2. In this calculation, the acceleration voltage of NBI is set to be 27kV and the electron density $\bar{n}_e$ is $2\times10^{19}m^{-3}$. The velocity distributions at the different radial positions from r/a=0.1 to 0.8 indicates the slowing down of the three energy components (full E, E/2 and E/3) of beam ions.

Figure 3 shows the calculated FICXS spectrum in the case of the sightline A. The resolution of the gyro-phase of the fast ion is set to be 20 degree. The red-shifted emission is expected since the angles between the sightline and the BL2 beamline is about 60 degree. As compared with the cold component of the H_α-line (656.3 nm), the spectrum in the wavelength range more than 658 nm is related to the fast ion (E > 10keV) component. Moreover, a folded spectrum can be seen at λ > 659.5 nm, which is due to the full energy component of the beam ions.

The previous anaysis of the halo neutral indicates that the halo neutral component is expected to be 50% of the beam component in the region of r/a < 0.7 [2]. In near futre, the spectrum comparison between the beam and halo components will be carrid out. For more precise calculation, we are applying a Fokker-Planck analysis code (FIFPC) to obtain the 2D velocity distribution of fast ions. This activity also help to forecast the fast ion distributions in the deuterium plasmas in LHD.

1) T. Ito et al., Rev. Sci. Instrum. **81**, 10D327 (2010).
2) S. Kobayashi, M. Osakabe, et al., Joint Conf OS2012 and PMIF2012, 2012.8.27-8.31 Tsukuba, Ibaraki, Japan, O-18.

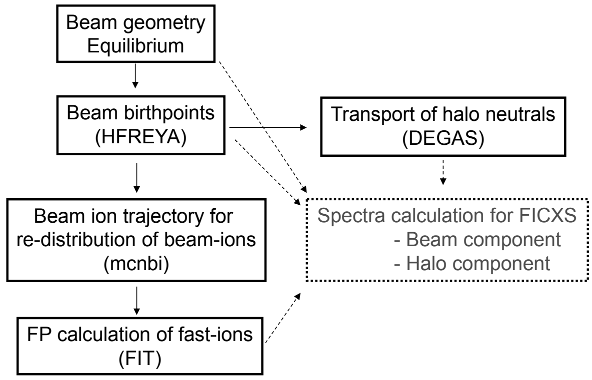

Fig. 1. Calculation scheme for the estimation of the fast ion charge exchange spectrum.

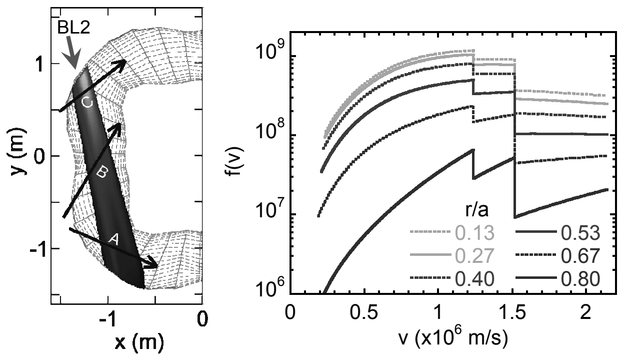

Fig. 2. (Left) 2-dimensional beam density of co (BL2) NBI and sightlines of the test geometry for the FICXS spectrum calculation and (Right) velocity distribution of fast ions at r/a = 0.1 to 0.8 calculated by the Fokker-Planck analysis.

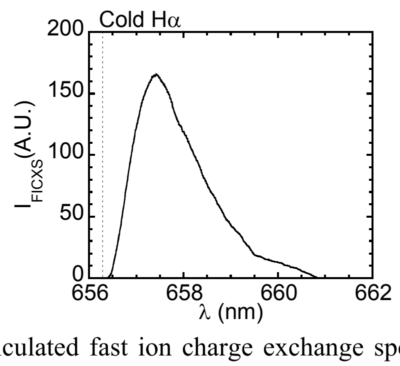

Fig. 3. Calculated fast ion charge exchange spectrum in the case of the sightline A. The geometry of the sightline is shown in the left figure of Fig. 2.